Российская Академия Наук

РОССИЙСКАЯ АКАДЕМИЯ НАУК

ИНСТИТУТ ПРОБЛЕМ БЕЗОПАСНОГО РАЗВИТИЯ АТОМНОЙ ЭНЕРГЕТИКИ

RUSSIAN ACADEMY OF SCIENCES

NUCLEAR SAFETY INSTITUTE

Препринт ИБРАЭ № IBRAE-2002-08

Preprint IBRAE-2002-08

M. Kanevski, E. Savelieva, V. Demyanov, S. Chernov, O. Sorokovikova, V. Belikov

SCIENCE-BASED MODELLING OF CHERNOBYL FALLOUT TREND

Москва
2002

Moscow
2002

УДК 502.3

Каневский М., Савельева Е., Демьянов В., Чернов С., Сороковикова О., Беликов В. ФИЗИЧЕСКОЕ МОДЕЛИРОВАНИЕ АТМОСФЕРНОГО ПЕРЕНОСА ЧЕРНОБЫЛЬСКИХ ВЫПАДЕНИЙ (на англ. яз.). Препринт № IBRAE-2002-08. Москва: Институт проблем безопасного развития атомной энергетики РАН, 2002. 23 с.

Аннотация

Данная работа посвящена физическому моделированию загрязнения ^{137}Cs вследствие Чернобыльской аварии. Чернобыльские выпадения представляют собой пример данных с нелинейным трендом и высокой локальной вариабельностью, и поэтому они очень эффективны для тестирования нелинейных методов оценки. Физическое моделирование атмосферного рассеяния выполнено с помощью лагранжевой модели атмосферного переноса и программного пакета «Нострадамус», разработанных в ИБРАЭ. Тем не менее, несмотря на тщательную предварительную подготовку параметров модели, в конечном результате было получена только основная ориентация чернобыльского следа. Модель не воспроизвела пятнистую структуру данных, представленную в измеренных точках. Такая ситуация вызвана неточным знанием параметров, важных для атмосферного моделирования – Чернобыльский пример показал, что он является слишком сложным для чистого физического моделирования. Невязки физической модели были изучены с использованием Искусственных Нейронных Сетей. Такая смешанная модель позволяет улучшить результаты, добавляя некоторые “горячие пятна”, расположенные не на основном чернобыльском следе.

Kanevski M., Savelieva E., Demyanov V., Chernov S., Sorokovikova O., Belikov V. SCIENCE-BASED MODELLING OF CHERNOBYL FALLOUT TREND. Preprint IBRAE-2002-08. Moscow: Nuclear Safety Institute RAS, 2002. 23 p.

Abstract

This work is devoted to the science based modeling of ^{137}Cs contamination due to Chernobyl fallout, this fallout is an example of data with non-linear trend and high local variability and that’s why they are very efficient for testing non-linear estimators. Science based atmospheric dispersion modeling is performed on the base of the Lagrange model atmospheric transport model and with the help of software NOSTRADAMUS, developed at IBRAE. Nevertheless of detailed preliminary preparation of model parameters the final result shows only the main orientation of the trace. It does not reproduce the spotted structure presented in measured data. Such situation is caused by not exact knowledge of parameters important for atmospheric modeling – Chernobyl example seems to be too difficult for pure science-based modeling. The residuals of science-based model were studied using Artificial Neural Networks (ANN). Such hybridization allows to improve the results by introducing some “hot spots” distributed not in the main trace.

Science-based modelling of Chernobyl fallout trend

M. Kanevski, E. Savelieva, V. Demyanov, S. Chernov, O.Sorokovikova, V.Belikov

THE INSTITUTE OF NUCLEAR SAFETY
113191, Moscow, B. Tulskaya, 52

tel.: (095) 955-22-31, fax: (095) 958-11-51, E-mail: esav@ibrae.ac.ru; http://www.ibrae.ac.ru/~mkanev

Contents

1 Introduction

Analysis and mapping of complex and spotted structure of a contaminator due to a fallout can be performed by one of different approaches:

a) science based modeling – an attempt to reconstruct the atmospheric dispersion of pollutants and their deposition and
b) data-driven modeling based on the real measurements of soil contamination in the region of interest.

This work is devoted to the first approach. Analysis are performed on ^{137}Cs contamination due to Chernobyl fallout, this fallout is an example of data with non-linear trend and high local variability and that's why they are very efficient for testing non-linear estimators.

Science based atmospheric dispersion modeling is performed on the base of the Lagrange model atmospheric transport model, developed at IBRAE. The model is used for the Chernobyl fallout reconstruction in a selected region. The modeling results heavily depend on the source term parameters (height of the release, temperature, etc.), meteorological fields (rainfalls, wind speed and direction). Wet deposition gives rise to the high level of contamination and "hot spots". To discribe correctly wet deposition (washout of the nuclides from the cloud) due to rainfall occurred in the region during the cloud traveling detailed reconstruction of the rainfall field is requered. The parameters of the source term and available meteorological information were seriously analyzed and prepared for usage in the atmospheric transport model.

The parameterization of the source – the height of release and its temperature – was performed on the base of some physical knowledge about the current source and according to different descriptions of Chernobyl accident. The rainfall field was reconstructed by using Kernel Regression Estimator (KRE) on the base of available meteorological data. The rainfield reconstruction was performed for special points in the space/time continuum (the spatial location in the time of contaminated cloud passing). The precipitation parameters were taken from corresponding inquiry-books.

The atmospheric dispersion modeling was performed with the help of software developed at IBRAE (NOSTRADAMUS).

Nevertheless of detailed preliminary preparation of model parameters the final result shows only the main orientation of the trace. It does not reproduce the spotted structure presented in measured data. Such situation is caused by not exact knowledge of parameters important for atmospheric modeling – Chernobyl example seems to be too difficult for pure science-based modeling. The residuals of science-based model were studied using Artificial Neural Networks (ANN). Such hybridization allows to improve the results by introducing some "hot spots" distributed not in the main trace.

2 Theoretical Description of the Physical Atmospheric Model

2.1 Description of the Lagrangian atmospheric transport model

The basis of the NOSTRADAMUS computer system forms the Lagrangian atmospheric transport model. In trajectory Lagrangian models, dispersion of the impurity cloud is treated as simultaneous motion of a great number of trial marks. When doing so, dispersion of the impurity in the atmosphere is simulated by means of some stochastic movement that is imposed on the regular transport of the marks, conditioned by the "mean" wind.

Stochastic models of atmospheric dispersion can be divided into two classes. The first one embraces trajectory models with random transport of particles in turbulent atmosphere. Models with random perturbations to velocities, determined from Langevin's equation, belong to the second class.

The models of the second class require considerable computational efforts. In the models, statistical characteristics of atmospheric turbulence are employed as input data. These models can be grouped with statistical ones.

The models of the first class are based on a simplifying assumption that the time scale of diffusion is much longer than the time of velocity correlation. As input data, they require specification of empirical coefficients of turbulent diffusion. These models are more economical and can be used on personal computers. The model being described here belongs to this type.

By now, the trajectory models of the first type have been subjected to a thorough methodical validation and for the time being are considered to be among the most promising numerical procedures for calculation of contamination dispersion in a non-uniform field of velocities.

The trial marks simulating the stream of contamination are emitted successively from the source in accordance with the source's intensity and each of the marks moves at the wind velocity at the point where this mark is located. Random deviations simulating the dispersion of the impurity in the atmosphere are superimposed on this motion. The value of the random deviations is in a certain relationship with the coefficient of turbulent mixing that depends on atmospheric conditions.

The numerical algorithm looks as follows. At a next-in-turn time step, the *i*-th mark exhibits a shift in response to wind transport:

$$dx_i = V_x \Delta t\,; \quad dy_i = V_y \Delta t\,; \quad dz_i = V_z \Delta t \tag{2.1}$$

$$V'_z = V_z + V_g + \partial K_z / \partial z \tag{2.2}$$

After that, each mark undergoes a random shift with a value of:

$$dx_i = (2K_y \Delta t)^{1/2}\, \xi\,, \; dy_i = (K_y \Delta t)^{1/2}\, \xi\,, \quad dz_i = (K_z \Delta t)^{1/2}\, \xi\,, \tag{2.3}$$

In the above formulas, dx_i, dy_i, dz_i denote the shifts along the axes x, y, z; V_x, V_y, V_z are the respective wind velocity components; Δt is the time step; K_y, K_z are the coefficients of turbulent diffusion in horizontal and vertical directions; ξ is a random quantity with normal distribution, unit variance, and zero mathematical expectation.

The velocity of regular motion in the vertical direction, V_z includes, along with the vertical wind component proper, two additional terms. The first one, V_z , is the gravitational drift rate that is non-zero, if one considers transport of aerosols (not gases), and depends on size, density and shape of the particles. For spherical particles, this rate is described by the Stokes formula.

The second term proportional to the vertical gradient of the diffusion coefficient appears in the case of variable K_v and is required to bring the density of particles moving in accordance with (2.1–2.3) in full correspondence with the basic equation of advection/diffusion. This term is not always taken adequately into account in similar models though disregard of these corrections may distort the results appreciably [1,2].

At present, a hybrid technique of "erratic clouds" is developed at IBRAE to solve a semi-empirical equation of turbulent diffusion. This technique combines the advantages of both Gaussian and Lagrangian models. The main idea of the technique is in parametric separation of atmospheric dispersion of an impurity into two processes, viz., random transport of the cloud center, and growth of cloud dimensions. The Puff- model and the model of random shifts of particles are particular extreme cases [3,4].

A modification of the ordinary trajectory model consists in that each of randomly moving marks is treated as a center of a separate cloud of the impurity with a Gaussian density distribution – analog of the cloud in the Gaussian model. The growth of dimensions of the clouds with time is governed by the diffusion law.

When doing so, the growth of the clouds and value of random shifts are chosen in such a way as to ensure accurate correspondence between the net dispersion of the cloud and the solution of the basic diffusion equation. It is provided by calculation of random shifts of the clouds using the following formulas:

$$dx_i=(2K_y\alpha\Delta t)^{1/2}\,\xi,\quad dy_i=(K_y\alpha\Delta t)^{1/2}\,\xi,\quad dz_i=(K_z\alpha\Delta t)^{1/2}\,\xi,$$

while the growth of cloud dimensions, using the formulas:

$$d/dt(R^2)=2K_y(1-\alpha),\qquad d/dt(H^2)=2K_z(1-\alpha),$$

where R is the horizontal cloud dimension; H is the vertical cloud dimension; α is the parameter of separation. For $\alpha=1$ we have an ordinary stochastic model and for $\alpha=0$ – the Puff-model. The density at a given point is determined by the sum of densities of all the clouds.

The use of such a hybrid technique allows to smooth out the results, which offers the possibility of employing a small number of the marks and thereby reducing the time calculation and saving the resources. This was one of the objectives pursued while developing the model. As a result, the code implementation of the model meant for capabilities of personal computers can be used for prompt prediction in real time scale (calculation of an option is 100 times shorter than the actual time of cloud dispersion).

When modeling dry fallout, the well known relationship between the near-to-surface radionuclide concentration in the air (C_X, Bq/m^3) and the fallout density (σ, Bq/m^2):

$$\sigma = v_{dry}\bullet C_x\bullet\Delta t$$

is used, where Δt is the time of cloud passage over the given point. In the case of wet fallout, the conventional formula

$$\sigma=\left(\int_0^H C(h)\cdot dh\right)\cdot\lambda\cdot\Delta t \text{ and } \lambda=d\cdot\vartheta^{\alpha}$$

where H is the altitude of rain clouds, which was assumed to be higher than that of the radioactive cloud in this case; and λ is the quantity inverse to the time of washout, was also employed, where d is a constant and the parameter α is different for different groups of radionuclides.

A detailed description of the model and numerical algorithm is presented in [5, 6].

2.2 Model description (plume rise and distribution of realize under the source)

If the heat source intensity can be considered quasi-stationary, the parameters of convective flow over the source quickly reach equilibrium. Let us assume that the shape and the extent of the cloud of trace species over the source with some initial buoyancy and momentum after some arbitrary time are the same as those of the cloud produced by the steady flow for the same period of time. In this case the concentration of release from steady source in height interval [Z,Z+H] is determined by the source intensity during the time the front of the convective plume was in this height interval. Let us formulate the equations of the time evolution of the convective plume front position. The plume trajectory is given by equations

$$\frac{d\,Z}{d\,t}=W \tag{2.4}$$

$$\frac{d\ X}{d\ t} = U \tag{2.5}$$

where Z is the height of the source, X is the distance from the source and U is the horizontal velocity of the stream (it can differ from the wind speed).
Equations for the speed are the following:

$$\frac{dW}{dt} = g\frac{T\ - T_0}{T_0} - \alpha W^2 \tag{2.6}$$

$$\frac{dU}{dt} = \alpha(U_0 - U\ )W \tag{2.7}$$

Equation for the temperature is as follows:

$$C_p\frac{dT}{dt} = -\alpha\ \ (T\ - T_0)C_pW - g\frac{T}{T_0}W \tag{2.8}$$

Equation for the effective radius of the plume is

$$\frac{2}{R}\frac{dR}{dt} = \alpha W(1 + T_0 / T) - g\frac{T\ - T_0}{T_0W} + \frac{g}{T_0}\frac{C_VW}{C_p(C_p - C_V)} \tag{2.9}$$

Equations (2.4)-(2.8) and equation (2.9) are used in the first time period of plume traveling, while $T \rangle T_0$ for a plume. After $T \approx T_0$ for a plume the next approximation for (2.9) is used – the vertical speed changes the sign and equation (2.9) is transformed in the form:

$$\frac{1}{R}\frac{d\ R}{d\ t} = \alpha\left|W\right| \tag{2.9'}$$

The expression for entraining has been used from [7], where the influence of the horizontal wind is taken into account:

$$\alpha = \frac{C}{R}\frac{T}{T_0}\sqrt{1 + (u / W)^2}$$

or

$$\alpha W = 1/\ M\frac{d\ M}{d\ t} = \frac{C}{R}\frac{T}{T_0}\sqrt{U^2 + W^2}$$

where *C=const.* Here the following notations are used: R is the radius of a plume, $T -$ temperature of a plume, T_0 is the temperature of the ambient air, which depends on an altitude, U is the horizontal speed of a plume, W is the vertical velocity of a plume, X is a horizontal coordinate of plume center trajectory, Z is a vertical coordinate of plume center trajectory, U_0 is atmospheric wind's speed, which depends on an altitude, C_p and C_v are air heat capacities under constant pressure and volume correspondingly and $M = \rho R^2W$.
While moving in the moist atmosphere the humidity of the plume changes up to condensation level by the following formula:

$$\frac{d\ q}{d\ t} = \alpha W(q_0 - q)$$

where q_0, q are specific humidity values of the ambient air and the air in a plume correspondingly.

T and T_0 are changing during the movement to the virtual temperatures. So, the equation (2.8) should be corrected for conditions of saturation due to appearance of a new heat source that is bounded up with condensation. But for the case of a plume containing great amount of water vapor the using of virtual temperature in this system of equation is not applicable. Full equations and the equation for enthalpy have to be used (2.8').

$$dU + P\,dV = 0;\quad U = M\cdot\varepsilon$$

$$d\,(M\cdot\varepsilon + P\,V) - V\,dP = 0;$$

$$d\left(M\cdot h\right) - \frac{M}{\rho}\cdot dP = 0,\quad h = \varepsilon + \frac{P}{\rho}$$

$$\frac{d\left(M\cdot h\right)}{dz} = h_0\,\frac{dM}{dz} + \frac{M}{\rho}\,\frac{dP}{dz};$$

$$\frac{dH}{dt} = C_{p0}T_0\,\frac{dM}{dt} + \frac{\gamma-1}{\gamma}\,\frac{H}{P}\,\frac{dP}{dt} \qquad (2.8')$$

where $H = C_p MT$ is an enthalpy, H_0 - enthalpy of the ambient air, γ - is an adiabatic exponent for gas mixture, $C_{p\,0}$ - is heat capacity of ambient air, $C_p = \sum C_p\,\rho_i \;/\; \sum \rho_i$.

The heat capacity of the dry air considered as independent from the temperature. The heat capacities of the condensed water and vapor are taken into account (*i* components of the mixture).

In vapor-filled plumes and in high-intensity conventional plumes the water vapor can condensate as temperature of the plume decreases. It happens if:

$$\rho_p \rangle \rho_n$$

where ρ_p . is a vapor density and ρ_n is a saturated vapor density.

In this case the condensed liquid water mass is dM_s. and the released energy is

$$dE = dM_s.Q,$$

where *Q* is a specific latent heat.

An amount of the condensed liquid water and new temperature is determined by iterative procedure. If convection is accompanied by condensation then there is a possibility of release to precipitate in the neigborhood zone. Some examples of using this model for estimation of the smoke injection of a height intensity fire release are presented bellow in Figure 2.1.

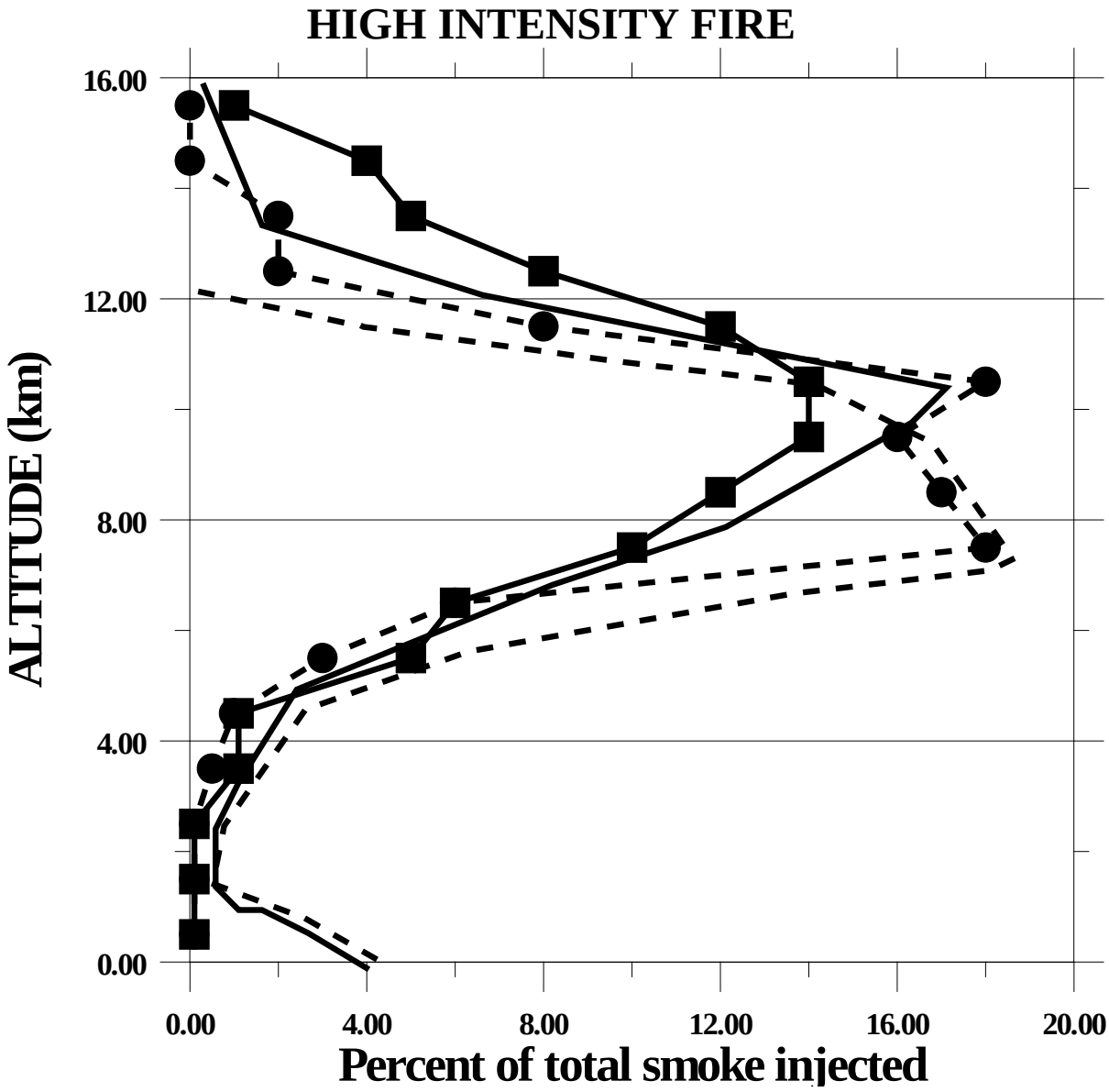

Fig. 2.1. Percent of total smoke injected at each altitude after 1h for a high intensity fire of source strength 890000W/m^2 [9] solid line -model (no water vapor) solid line with marks -3D Livermore Laboratory model (no water vapor) dots -model (with water vapor) dots with marks -3D Livermore Laboratory model (no water vapor)

2.3 Model closure constants

The validation of models requires their results to be consistent with the experimental datasets. The constants necessary for the model closure are determined during model validation. As data for validation were used Briggs formulas constructed for the cases based on numerous observations. Briggs approximation is based on a big set of experimental and environmental data obtained in several situations. The most studied are cases with conditions of stable and uniform stratification in the layer of convection [7]. The results under the stable stratification are obtained:

- for jet and low wind speed;
- for buoyant plume under low wind condition;
- for the final height of bent-over buoyant plume.

The other case studies used for model validation are:

- cooling tower data, for the sources of big area but small intensity;

- wood and oil-field fire data, for the powerful source cases when the final height is above the mixed layer. The corresponding data are presented in [8].

The results were also compared with the results of the 3-dimensional hydrothermodynamic model.
At the present time the 3-dimensional model RAMS (Regional Atmospheric Modeling System) of Colorado State University and the Livermore Laboratory model is used to simulate the convective fluxes over the fire source [7-13]. All of them take into account the latent heat of evaporation.
The studies [1,3,5,6] contain information on fourteen numerical experiments on simulation of convective streams over intensive heat release source. As a result of these numerical experiments, the values of the model closure constants have been obtained.
Estimation of coefficient in accordance with validation study is the following:
When the vertical speed of a plume is much bigger then the ambient wind speed (U/W ≈ 0)

$$C=0.15 \tag{2.10}$$

This is in agreement with the data from [7].
For the bent-over part of plume and jet, in any case when vertical velocity becomes equal or smaller then the horizontal one 0<W/U<1, the entrainment constant increases significantly.

$$C=0.9 \tag{2.11}$$

This is in agreement with the data from [7]
In the case, if the ratio of horizontal velocity to the vertical one 0<U/W<1, the linear interpolation between values (2.10) and (2.11) is used. Thus, the entrainment intensity varies with height, in agreement with observations.

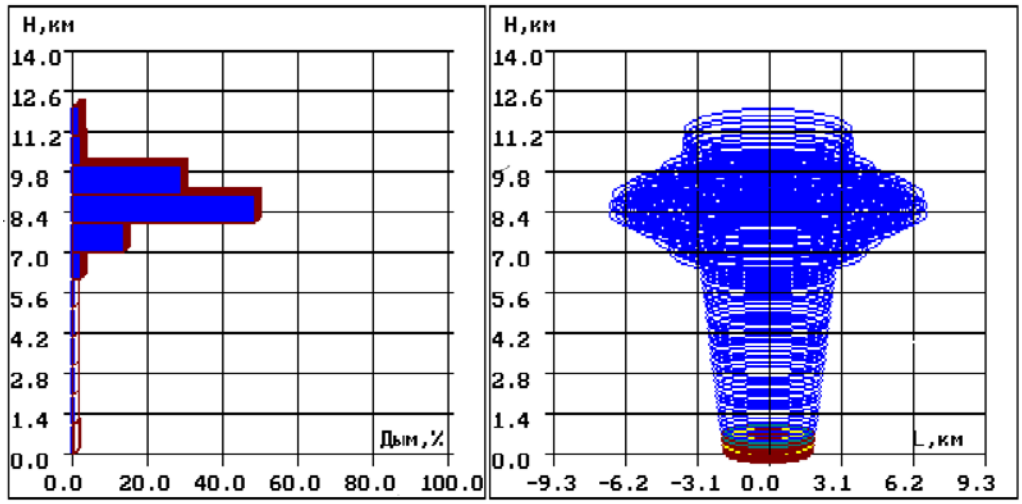

Fig. 2.2. The view of smoke column and smoke propagation with height for Hamburg fire.

2.4 Description of the NOSTRADAMUS computer system

From the very beginning, the "NOSTRADAMUS" computer system has been developed as a system for prompt prediction, capable of operating in real time scale and intended for incorporation in decision making support systems in emergency situations.

Using the system in a situation of emergency, the most laborious operation is input of initial data. Therefore, the possibility of prompt (real time scale) handling of the arriving information on source of contamination and the meteorological situation should be provided, followed by processing of such information and its use for refining the prediction.

The requirement of real time scale reception and processing of diversified information from different sources leads to the necessity of distributing this work among a number of working places for the purpose of parallel and independent execution of operations.

As a whole, the system is subdivided into several independent subsystems (modules), which can operate in a parallel and autonomous mode in a local computer network.

The current version of the system consists of five subsystems:

- Module of control, coordination and preparation of general function information for all system components.
- Module of meteorological data preparation.
- Module for preparation of data on the source.
- Module of radionuclide dispersion prediction and radiation situation determination.
- Module of situation analysis on the basis of predictions and delivery of recommendations on countermeasures and data for decision making support.

All the modules exchange information through a common data bank via local network.

Input information for modules of source data preparation comes from "outside". The output information, irrespective of the volume and nature of the input data, is always represented in a standardized form and includes all data required for calculating the atmospheric transport of impurities. As this information is being prepared, it is transmitted over to the common bank of scenarios.

This information is read from the common bank in the module of predictions and used by this module for calculation of concentrations and fallout densities. The output data prepared by the module are stored in the common bank as a scenario. In its turn, the output data is then read by the module of countermeasure analysis and employed for preparing the output information to be sent "outside".

As soon as new, refined data on the atmosphere condition or the source appear in the common bank, more accurate predictions and countermeasure analyses are elaborated.

In the course of the session, all created variations are stored and operation of each subsystem is recorded with the purpose of subsequent analysis of the work performed by expert operators.

Such arrangement of the computer system allows to execute in parallel the most laborious functions of receiving and processing of "external" data, which enables to perform this work simultaneously and calculate dozens of prediction variations on real time scale.

The promptness of source data input is provided as well owing to the envisaged possibility of selecting some variations prepared beforehand and stored in the database. Such data can be adjusted and inputted with any desired degree of details.

While inputting information, its correctness is checked as early as possible and represented in the form of plots, level lines, vector fields, etc. for visual descriptive control.

Output of information is carried out against a locality map background in a maximally concentrated way, convenient for persons responsible for decision making. For example, different colors are employed for marking the zones corresponding to different decision making criteria (intervention levels). If a list of inhabited localities is given out, their names are illuminated to reflect the degree of risk associated with doses expected in the localities.

The system operates under MS Windows '95 environment and has a friendly interface implemented according to MS Windows standards.

3 Application of Physical Atmospheric Model to Chernobyl Fallout

3.1 Analysis of meteorologic parameters for atmospheric transport modeling

Input parameters for NOSTRADAMUS are parameters of the source and meteorological parameters (wind and rainfall). The first step was devoted to choose the meteorological parameters – rainfall field. At this stage the traditional parameters of the source were used. They are based on studies accomplished at an early stage of the accident. Simultaneous investigation of relatively intricate synoptic conditions made it possible to tie, with a sufficient certainty, the greater part of traces formed in the territory to the time of contamination and possible average altitude of radioactive cloud movement. In particular, the contamination of the northern part of the Gomel Region, south-eastern districts of the Mogilev Region, and the western part of the Bryansk Region occurred in the afternoon of April 28, 1986 as a result of releases from the reactor in the period from about 06:00 a.m. till 03:00 p.m., April 27, that is, in the period of the highest heat up of the core (according to the eye witnesses who observed the damaged reactor from a helicopter as well as those who saw the fire at the night of April 27). The dispersion of the radioactive tongue took place in a layer of 100 to 600 m above the earth surface, the tongue nucleus moving at an altitude of approximately 960 mbar (450 m above the sea level or 250-300 m above the earth) [14].

The initial movement of the radioactive tongue was due to north-west, which changed gradually to north by the night and later, after a turn, the clouds started their movement eastwards at an ever increasing rate. As a result of this turn, the very first streams (if the count is started from 00:00 27.04) that nearly reached Minsk followed through the center of the Mogilev Region, southern parts of Smolensk and Ryazan Regions, and, in a sufficiently washed-out condition, reached Tula and later Ryazan Regions. The streams that followed (starting from about 06:00 a.m., April 27) made a turn to the east at the boundary of the Minsk Region and after this moved a little further to the south. Subsequent streams followed ever narrowing loops, but all of them, produced before noon, April 27, rounded Gomel in the north. Starting from the noon, the radioactive tongue did not reach the latitude of Gomel and was moving eastwards, slightly touching the south of the Bryansk Region.

Table 3.1. Reconstruction of the trajectories for plumes of radionuclides issued from the distracted reactor on 27 of the April 1986

The elevation of the source – atmospheric pressure 960 Gpa,
450 m over sea,
200 m over surface

		Trajectory 2			Trajectory 3			Trajectory 4			Trajectory 5	
		latitude	longitude		latitude	longitude		latitude	longitude		latitude	longitude
27.04.86	3:00											
	6:00	**51,40**	**30,13**									
	9:00	51,62	29,86	8:00	**51,40**	**30,13**						
	12:00	51,83	29,48	11:00	51,62	29,84	10:00	**51,40**	**30,13**			
	15:00	52	29,05	14:00	51,79	29,44	13:00	51,48	29,78	12:00	**51,40**	**30,13**
	18:00	52,1	28,57	17:00	51,9	29	16:00	51,55	29,42	15:00	51,48	30,00
	21:00	52,2	28,2	20:00	52	28,7	19:00	51,75	29,16	18:00	51,57	29,80
28.04.86	0:00	52,4	28,03	23:00	52,14	28,46	22:00	52,00	29,00	21:00	51,74	29,59
	3:00	52,69	27,89	2:00	52,31	28,4	1:00	52,18	29,00	0:00	51,90	29,65
	6:00	53	27,9	5:00	52,55	28,44	4:00	52,29	29,10	3:00	52,02	29,84
	9:00	53,27	28,3	8:00	52,83	28,45	7:00	52,42	29,37	6:00	52,12	30,18
	12:00	53,45	29,3	11:00	53,07	28,9	10:00	52,49	29,76	9:00	52,20	30,82
	15:00	53,5	31,3	14:00	53,1	29,6	13:00	52,55	30,16	12:00	52,32	31,71
	18:00	53,4	33	17:00	53,16	31,6	16:00	52,61	30,60	15:00	52,30	33,20
				20:00	53,12	33,34	19:00	52,65	31,13			
29.04.86							22:00	52,56	32,6			
Total:	Ci			Ci			Ci			Ci		
	200000			200000			150000			100000		

Here we considered the migration of the radioactive materials released from the reactor from 06:00 a.m. till 03:00 p.m., April 27, 1986. In accordance with the character of the movement in the near field (30 to 100 km) where formed axial lines could be observed, four “conditionally stable” trajectories of movement were considered. For each trajectory, the coordinates of the pseudo-nucleus of the clouds were reconstructed (see Table 3.1).

The atmospheric stability of class D (neutral condition) was assumed for the whole time of plumes migration.

For rain reconstruction were available data presented in Fig. 3.4. There are selected data both from meteorological stations (19 samples containing also information on duration of the rain) and agricultural stations (providing only integrated estimation of mm). The whole number of sample locations is 189 overall the large region (530×285 km). Their distribution is not homogeneous and there are lots of zero value points. So rainfall reconstruction appears to be very difficult problem.

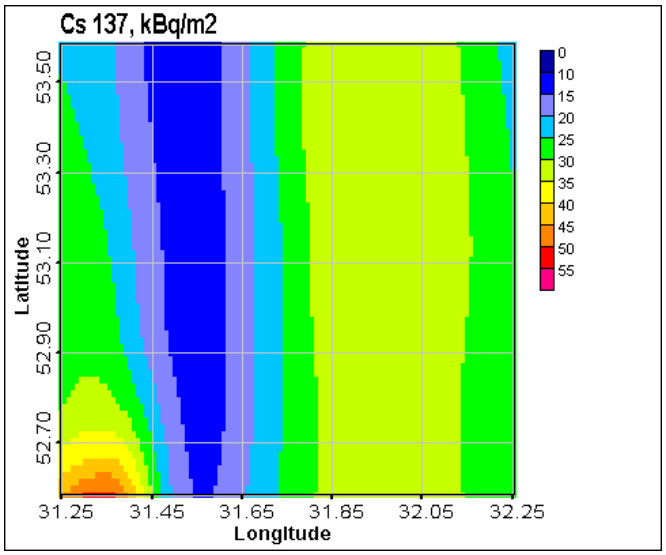

Fig. 3.1. Prediction mapping by Nostradamus without precipitation

a)

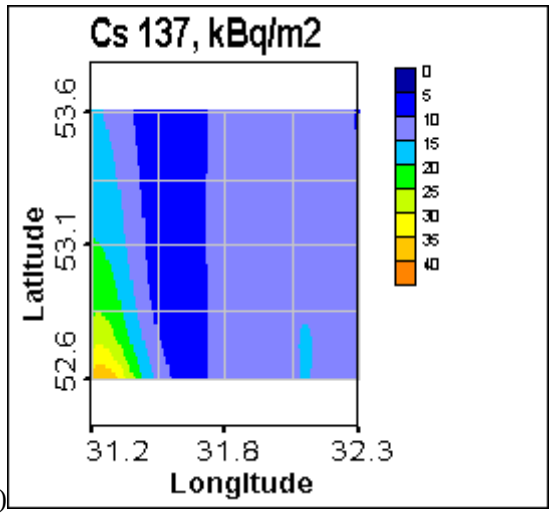

b)

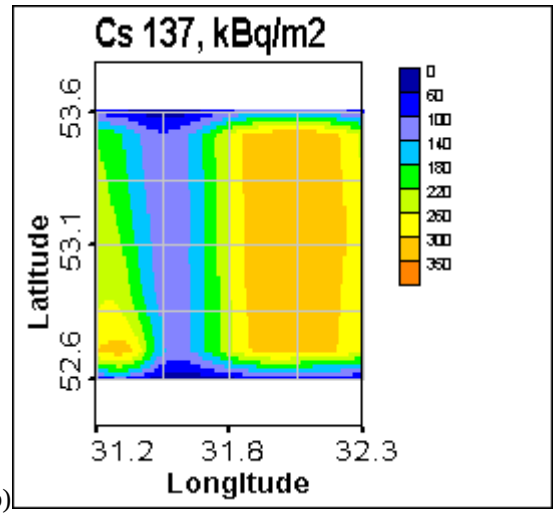

Fig. 3.2. Prediction mapping by Nostradamus with constant precipitations 1 mm/hour: a-over all region of cloud passing, b – over the region under study

General Regression Neural Network (GRNN) – one of realizations of Kernel Regression Estimator (KRE) – was used for rainfall mapping. The results obtained by GRNN are presented in Fig. 3.5. They are already selected so to satisfy the transport model – rainfall for the time of cloud passing. The results obtained by NOSTRADAMUS using reconstructed rainfalls are more similar to the data of surface contamination measurements (see Fig. 3.6) – they present spotted structure and positions of spots correspond with measurements. But the values of the model are very much lower.

Finally, the scenario of atmospheric stratification variability was changed. Recently the stable condition was used only during the nights. During the daytime the atmospheric stratification of class A was used.

a) 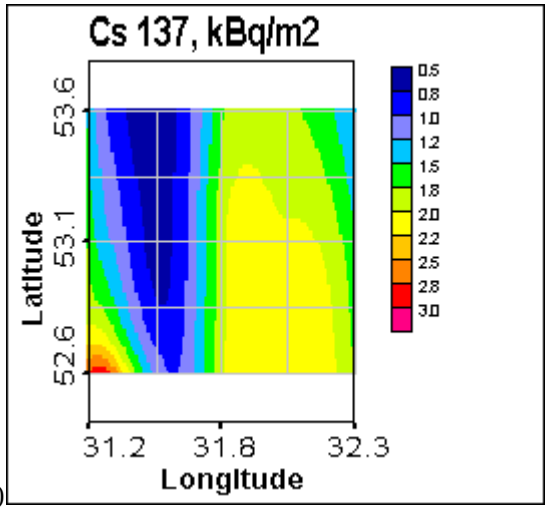

b) 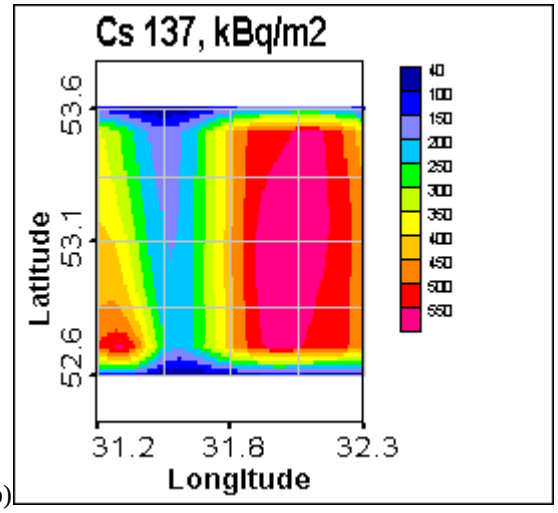

Fig. 3.3. Prediction mapping by Nostradamus with constant precipitations 2 mm/hour: a-over all region of cloud passing, b – over the region under study

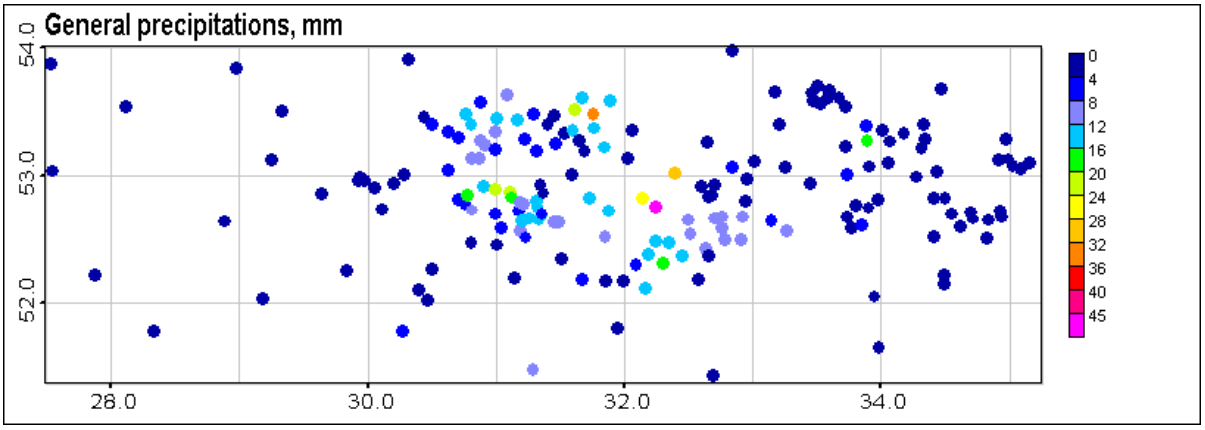

Fig. 3.4. Generalized data on the precipitations, mm

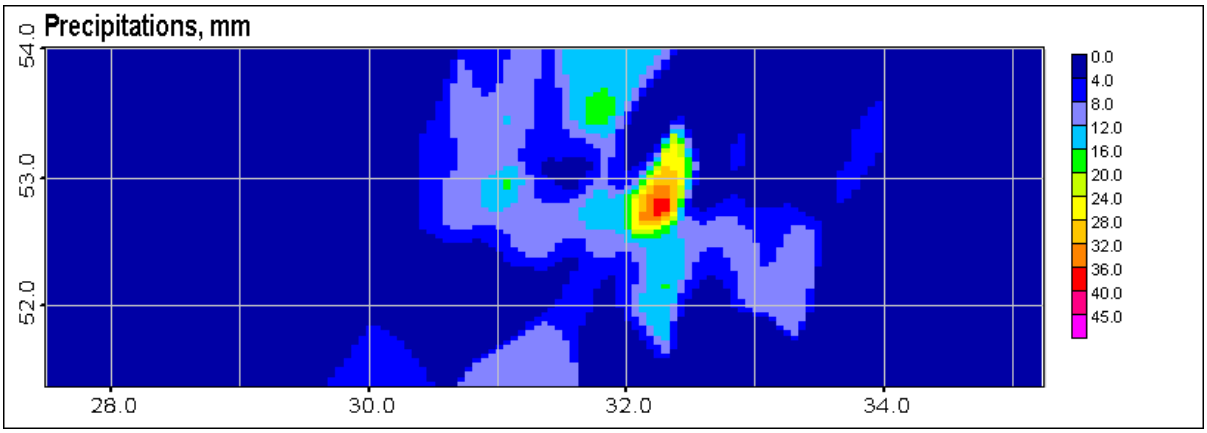

Fig. 3.5. Prediction mapping by GRNN model for precipitations, mm

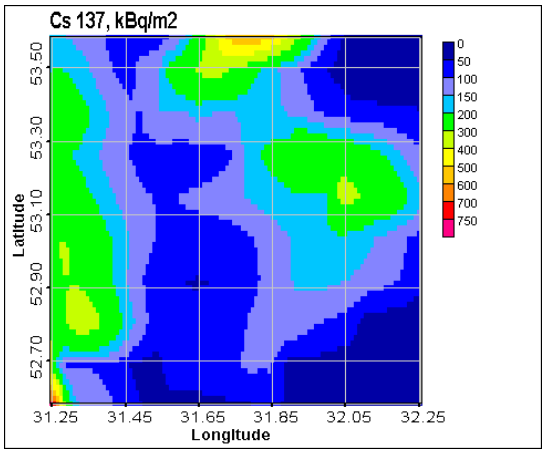

Fig. 3.6. Prediction mapping by Nostradamus with spatially distributed precipitations

3.2 Analysis of source parametrization

Preliminary results concerning atmospheric dispersion modelling of radionuclides' fallout (washout due to rainfall) were present above. There is very low correspondence between measured data and results of modelling. Firstly, the modelling provided very low concentration of radionuclides dispersed in region under study.

This part is devoted to find the more realistic scenario for initial height distribution of nuclides' release. For this purpose the information about heat of the release in the source, the model for plume rising and the distribution of release above the source was used. The theory is discussed in details in sections 2.2 and 2.3.

Different trajectories of radionuclide traces (see Table 3.1) are associated with different initial height of the release:

- The longest trajectory is corresponded to the height of release of maximum concentration of radionuclides equal to 1020m. It is up to the first hours after the accident.
- The second trajectory began with the height of maximum concentration of radionuclides in the cloud equal to 700m.
- Third trajectory had the height of maximum concentration of radionuclides release in the cloud 500m.
- The last trajectory corresponded the height of release equal to 300m.

According to the existing estimates made by an expert, the intensity of heat release during the first hours and days after the Chernobyl Nuclear Power Plant accident was:

source parameters

- first hour: from 7% to 2% of full power of source (3200Mv);
- next day: approximately 0.7% of full power of source;
- Temperature about 1500 ^{o} C;
- Effective radius of source about 9 m.

The data about winds in the region of power plant for the same period is:

meteorology

- first hour: low wind conditions ;
- next day: wind about 3m/s.

There is no data about gradient of temperature of ambient atmosphere at the moment of the accident, so the climate value (April) for Kiev (about 6^{o}/km) was used.

Results of modeling:

- First hour (7% of full power of source - 3200Mv)
  HEND= 1019 m – the height of maximum concentration of radionuclides in the cloud).
  Size of the cloud – top - 1100m; bottom - 700m.
- Next day (0.7% of full power of source - 3200Mv, wind about 3m/s)
  HEND= 470m – the height of maximum concentration of radionuclides in the cloud.
  Size of the cloud – top - 501m; bottom – 447.

3.3 Discussion of atmospheric modeling results

Results obtained by Nostradamus program using new source term parameters and atmospheric parameters are presented in Fig. 3.7. The general trend of ^{137}Cs contamination can be observed in it. This trend is the result of

traveling and dry and wet deposition of 4 clouds, released at different time and with different initial parameters (see discussion above).

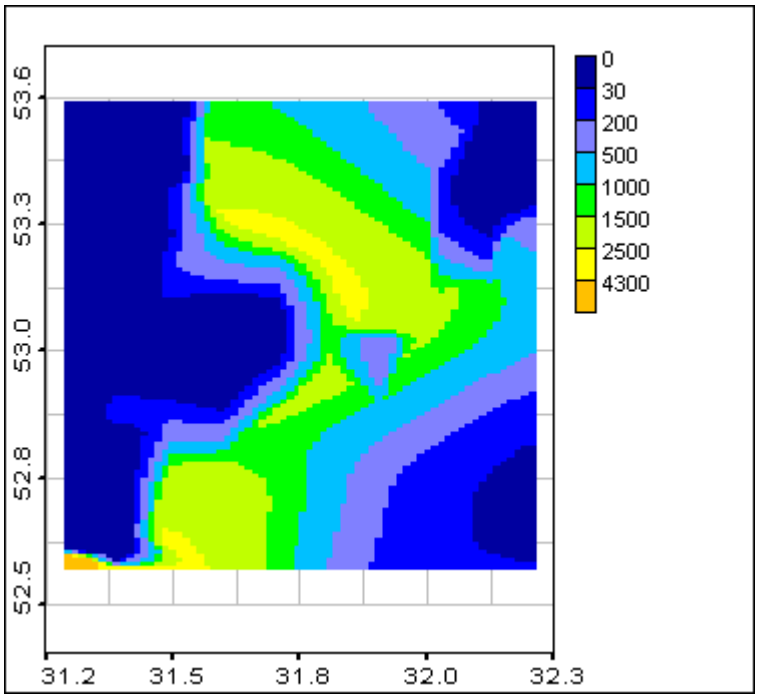

Fig. 3.7. Prediction mapping by Nostradamus with spatially distributed precipitations and physically based source term parameters

The results of ^{137}Cs fallout after physical atmospheric transport modeling were visually compared with real measured ^{137}Cs soil contamination. For this purpose the grid center the closest to a sample point was considered as an estimate for the sample location. The comparison is presented in Fig. 3.8 on Voronoi polygons using the same scale. The level of contamination (min and max) and the main form of the fallout of the model results and measured data are similar. The model results are a little more dissipated. Also the model does not present the spot in the west. In general atmospheric simulation estimates of the radioactive concentration on the surface show fair agreement with the data in the scale and basic overall shape of the pattern.

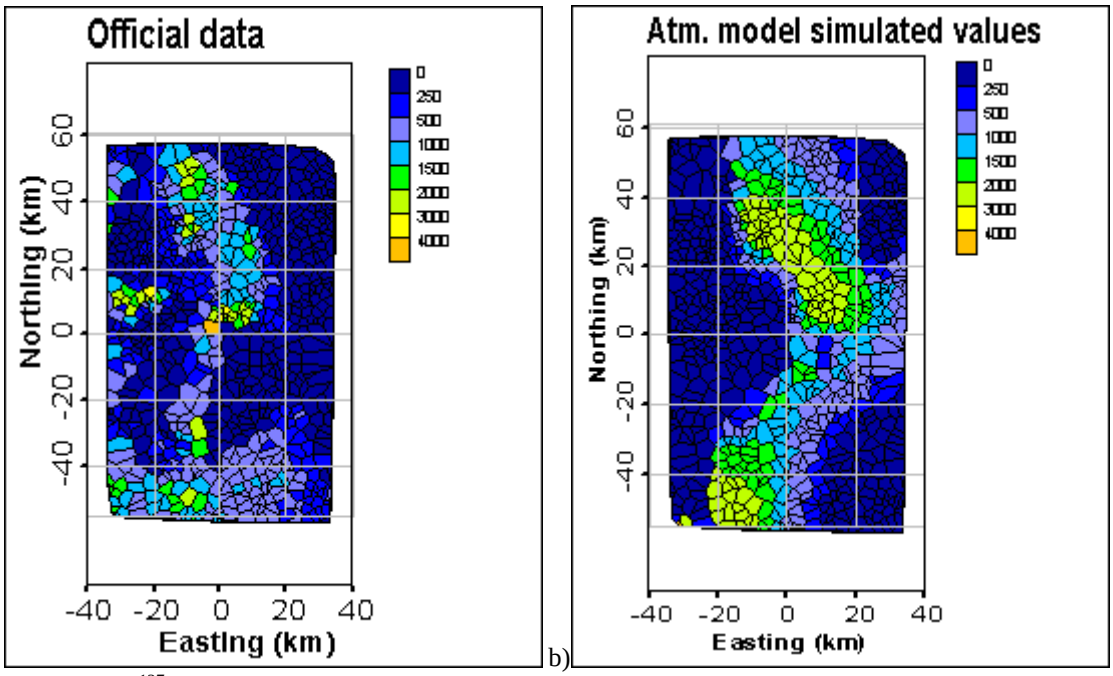

Fig. 3.8. ^{137}Cs concentrations: measured values (a) and simulated by the atmospheric model (b)

To look closer into the results of atmospheric model the scatter plot of the simulated vs. measured values at the original sampling locations is constructed (see Fig. 3.9). A few problems with matching the atmospheric model results with the actual sample pattern can be observed.

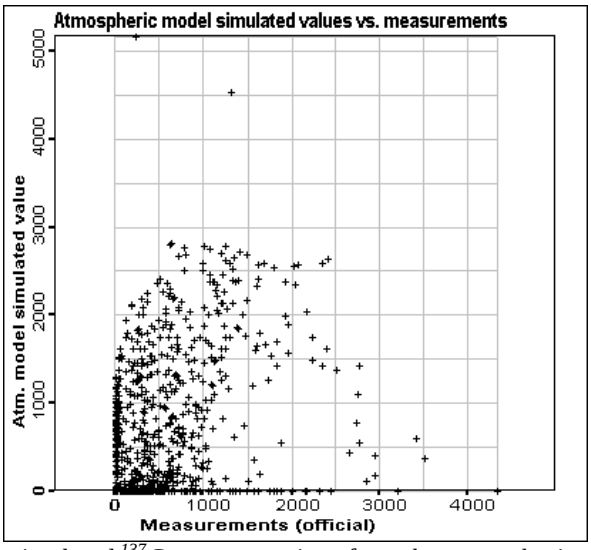

Fig. 3.9. Scatterplot of the simulated ^{137}Cs concentrations from the atmospheric model vs. measured values (official data)

The residuals (estimated value – real value) show some correlations with the official data (see Fig. 3.10 and 3.11). The distribution of the atmospheric model residuals (see Figure 3.10) shows high overestimation in the main trace caught by the model and high underestimation in small spots around it.

Preliminarily variogram analysis shows that atmospheric model simulated strongly correlated spatial pattern with smaller nugget and greater sill than the sample data (see Fig. 3.12). However, the overall variance level and basic correlation range was matched with the ones of the sample data. Nevertheless the residuals remain correlated with the same range as the sample data. This concludes that current atmospheric model was able to extract some correlation pattern but the ones left still features spatial correlation on the same scales, but at weaker level. So, current simulations cannot be treated as a justified trend model at any scale.

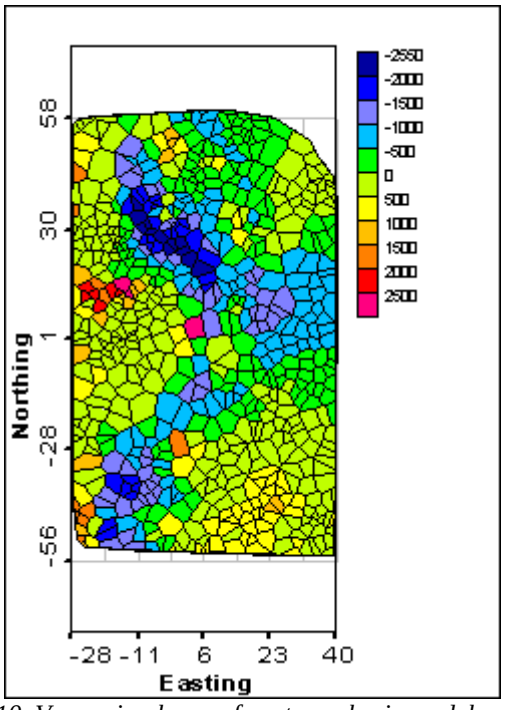

Fig. 3.10. Voronoi polygons for atmospheric model residuals

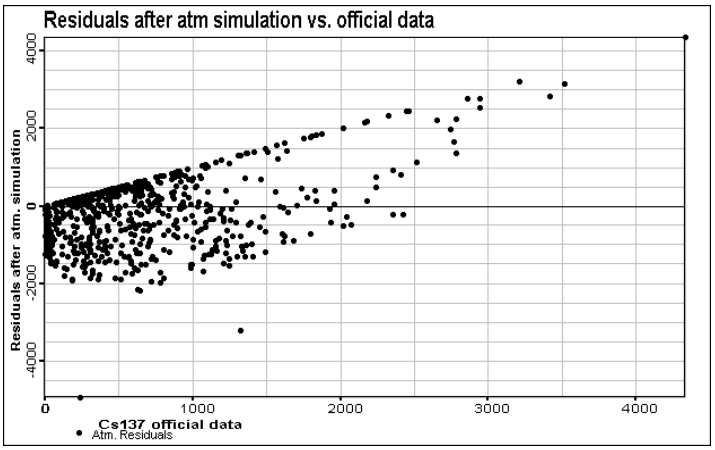

Fig. 3.11. Scatter plot of the residuals between measured (official) values and the simulated ^{137}Cs concentrations from the atmospheric model vs. the samples themselves

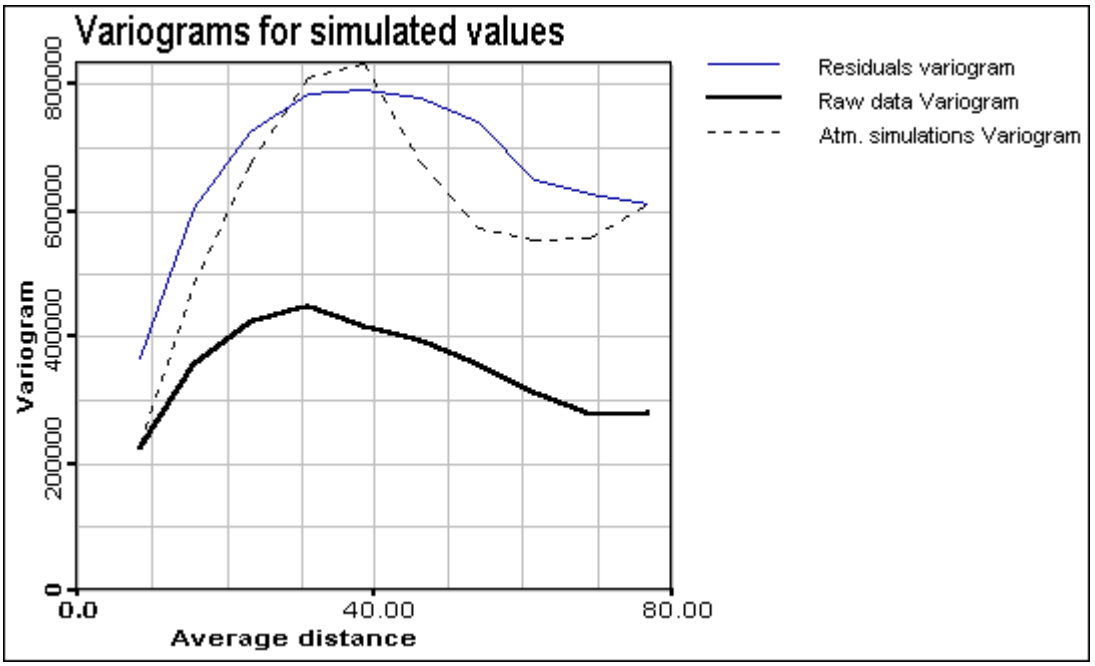

Fig. 3.12. Omnidirectional variograms of the sample (official) data, simulated values from the atmospheric model and the residuals between them

Statistical characteristics of residuals are gathered in Table 3.1 and presented as a histogram (see Fig. 3.13) and as a box-plot (see Fig. 3.14). The residuals are non-symmetric – there is more overestimations then underestimations (see Fig. 3.13 and difference between mean and median in Table 3.1). In 5 locations residuals may be considered as outliers and extremes (see Fig. 3.14).

Table 2.1. Statistical characteristics of the atmospheric model residuals

Min	¼ Q	Median	¾ Q	Max	Mean	Std. Dev.	skewness	kurtosis	MSE
-2528	-597	-15.9	284	3284	-157.4	790.3	0.05	1.7	648439

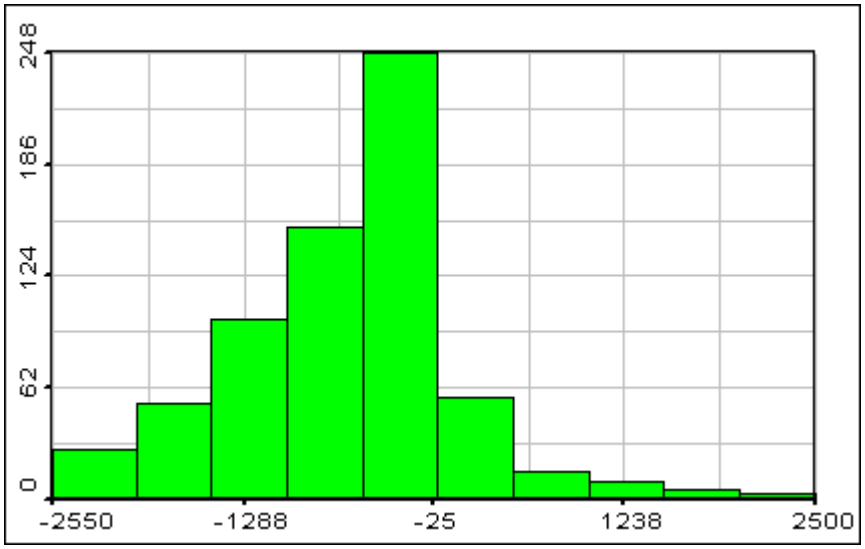

Fig. 3.13. Statistical histogram of atmospheric model residuals

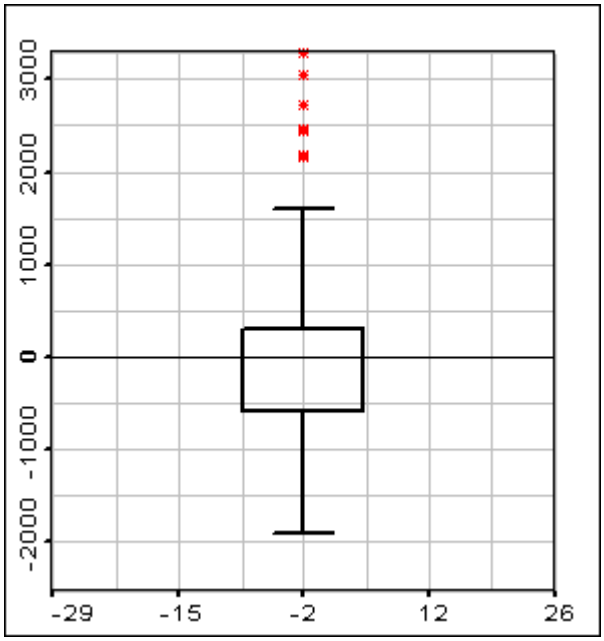

Fig. 3.14. Box-plot of atmospheric model residuals

4 ANN estimation of science based model residuals

The distribution of atmospheric model residuals has a visible structure (both in spatial distribution and in spatial correlation structure), which can be modeled using data driven models. Such approach can be treated as science based modeling of expected contamination due to a release with some fitting of a model after some real contamination measurements have been made. So it can appear to be interesting for after accident calculations.

In our case two different Artificial Neural Networks (Multilayer perceptron and General Regression Neural Network) are used as data driven methods to deal with atmospheric model residuals. The theoretical description of ANN approach can be found, for example, in [15].

4.1 Multilayer perceptron for atmospheric model residuals

To model atmospheric model residuals MLP with 2 inputs (coordinates), 2 hidden layers with 10 neurons in each and one output (real known residuals in sample locations) was used. The whole data set of measurements was partitioned into two sub-sets – one for MLP learning (training data set) and another for testing during learning

procedure (testing data set). The testing data set is important to prevent overfitting (early stop methodology – learning is finished when the error on testing data set begin to grow monotonically). Learning was performed by using Levenberg-Marquart gradient method after initial weights shaking with the help of genetic algorithms. The training procedure was stopped, when training error achieves value 0.001686. The testing error at that moment was 0.04581. The continuing of training procedure led to growing of testing error and, thus, to decreasing of MLP generalization ability.

Modeled residuals are presented in Figure 4.1. They are similar to raw residuals of atmospheric model (compare with Fig. 3.10). Spatial correlation of residuals modeled by MLP was compared with spatial correlation structure of initial residuals. Their correspondence (in general the level of variability) can be seen in omnidirectional variogram (Fig. 4.2).

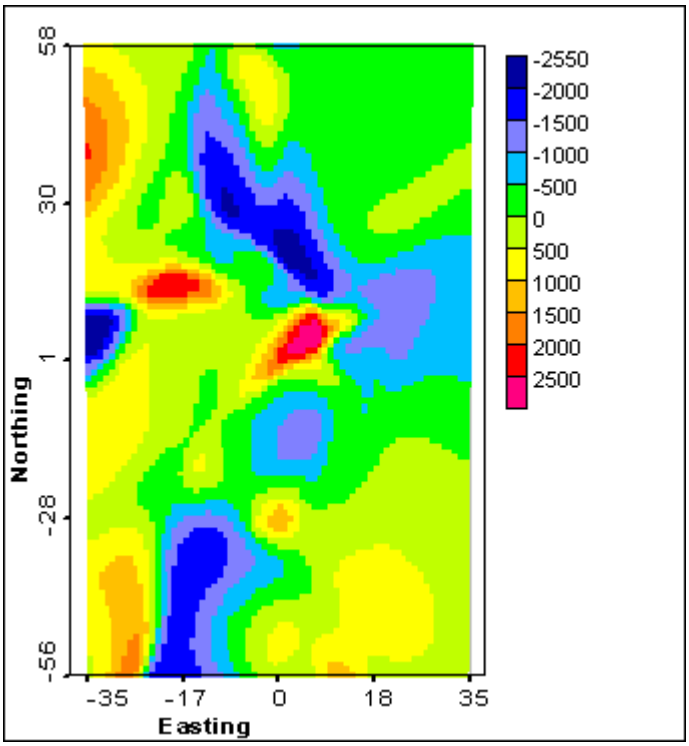

Fig. 4.1. Atmospheric model residuals modeled by MLP

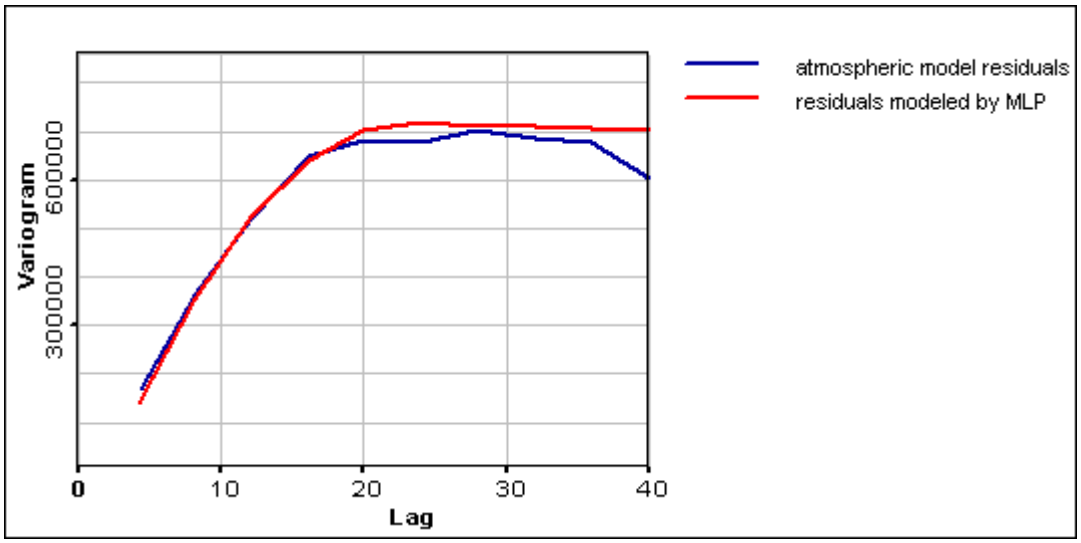

Fig. 4.2. Omni-directional variograms of atmospheric model residuals

The results of hybrid model – science based model précised by data driven model (atmospheric modeling + MLP) are presented in Fig. 4.3. Using MLP to residuals allowed to catch several spots left by atmospheric model. Some statistical test of obtained results was performed: level of data variability and range of correlation were

checked by omnidirectional variograms (see Figure 2.10); main statistical characteristics of hybrid model are gathered in Table 4.2.

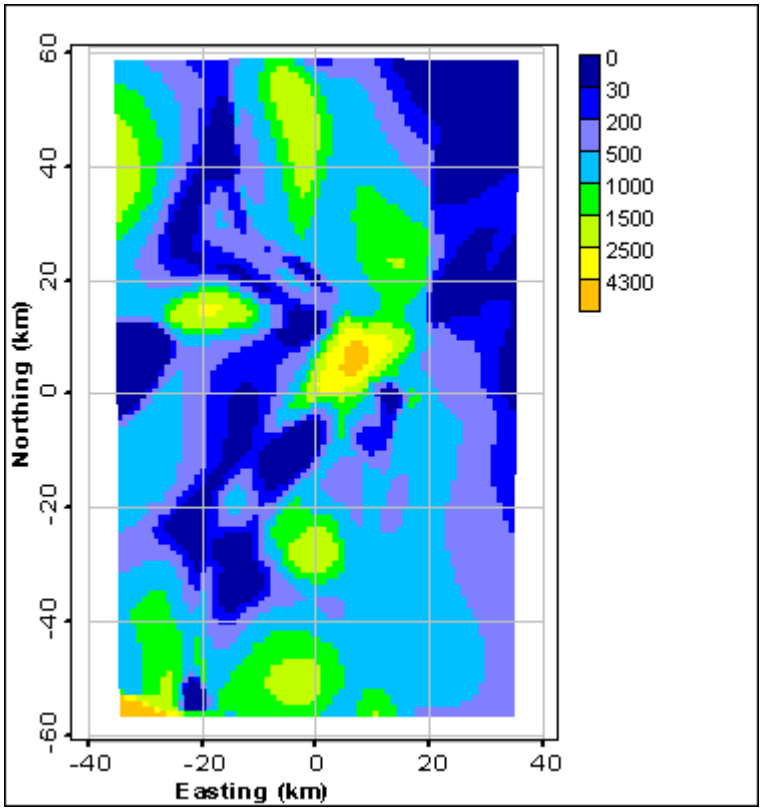

Fig. 4.3. Result of hybrid model: Atmospheric model + MLP 2-10-10-1 of residuals

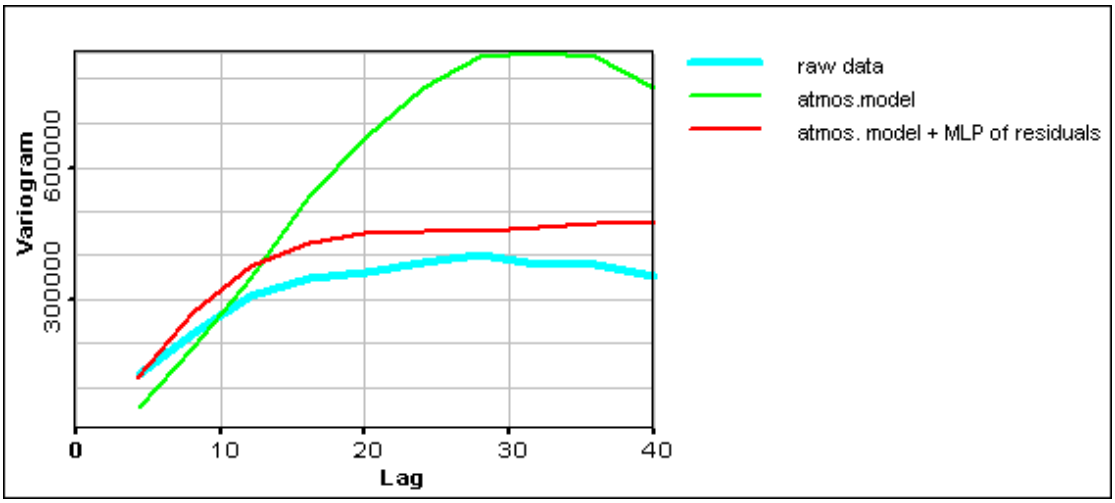

Fig. 4.4. Omni-directional variograms of atmospheric and hybrid with MLP models

4.2 General Regression Neural Network for atmospheric model residuals

GRNN was learned using cross-validation approach with final fitting by gradient search. Obtained parameters are presented in Table 4.1. Result of GRNN modeling of residuals is presented in Fig. 4.5. GRNN provides rather smooth result, the level of residuals' variability is underestimated (see Fig. 4.6). But general view of the residuals' pattern is very similar to initial one.

Table 4.1. GRNN parameters for atmospheric model residuals modeling

Sigma _X	Sigma_Y	Orientation	Training error
1.48	2.21	4	0.02

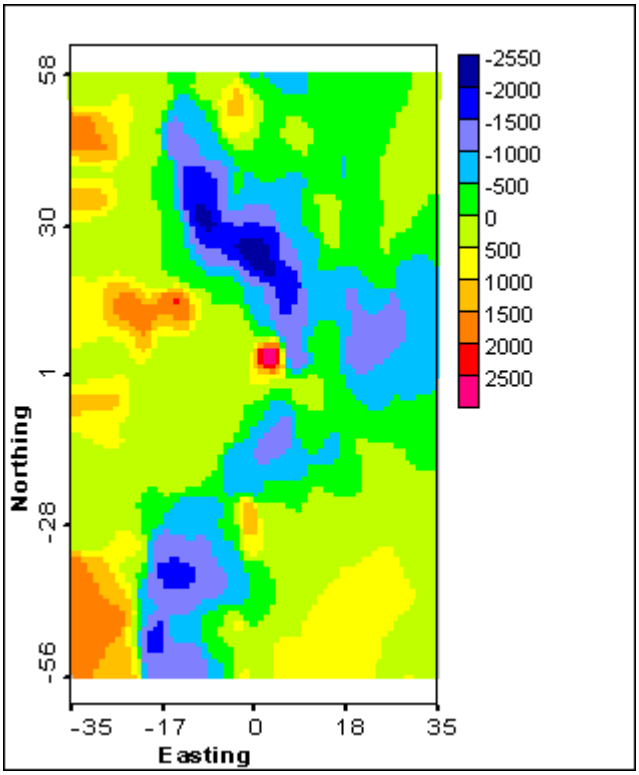

Fig. 4.5. Atmospheric model residuals modeled by GRNN

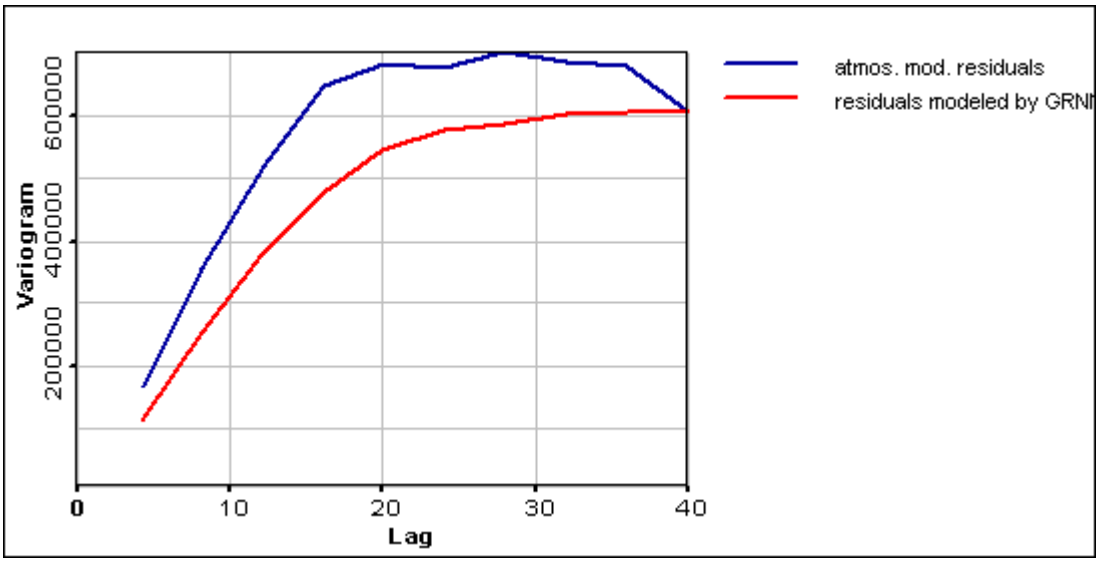

Fig. 4.6. Omni-directional variograms of atmospheric model residuals

As GRNN underestimates the level of variability, hybrid model with GRNN provides less level of variability of the final result (see Fig. 4.7).

Statistics of pure atmospheric model and hybrid models (atmospheric model + ANN) are gathered in Table 4.2 It can be seen that the best distribution is provided by atmospheric model combined with MLP. But MLP training is more difficult and not stable. So, as GRNN improves results it is safer to use it as a more stable method.

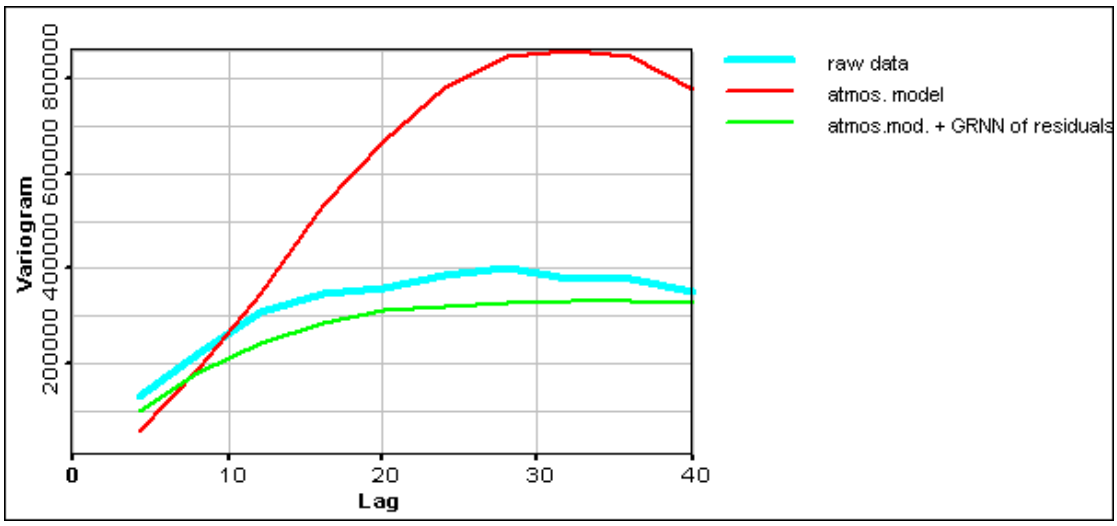

Fig. 4.7. Omni-directional variograms of atmospheric and hybrid with GRNN models

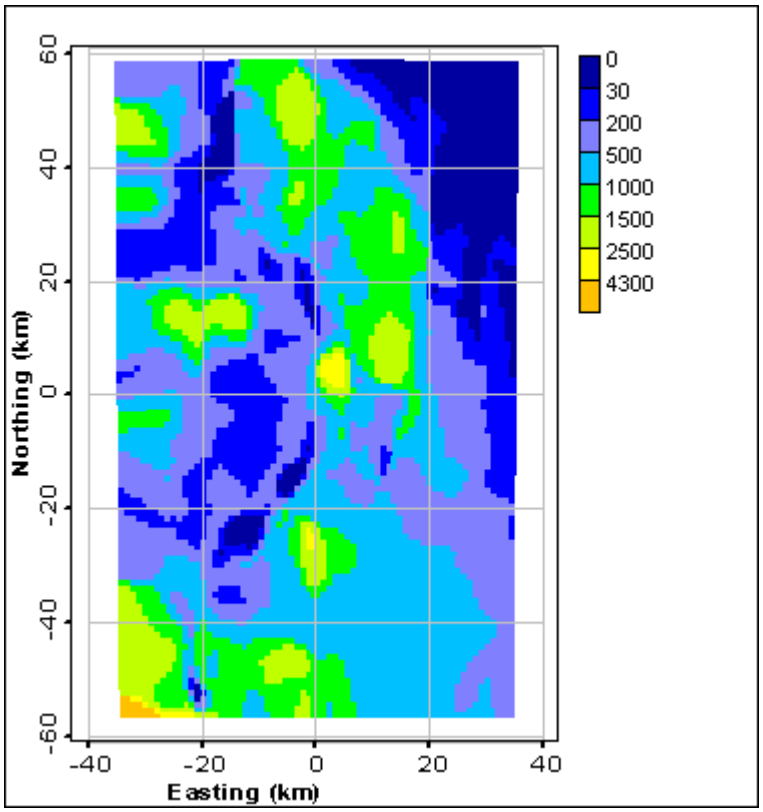

Fig. 4.8. Result of hybrid model: Atmospheric model + GRNN of residuals

Table 4.2. Statistical characteristics of atmospheric model and after modeling of residuals

	Raw data	Atmos. model	Atmos. model + MLP	Atmos. model + GRNN
Min	5.9	0	0	0
¼ Q	185	1	164.6	215.48
Median	382	346.5	523.82	503.43
¾ Q	801	1194	873.48	923.43
Max	4330	5233	5732.4	6793.48
Mean	571.72	678	633.46	639.13
Std. dev	561.4	783.8	650.78	593.53
Skewness	1.82	1.19	2.74	2.9
Kurtosis	4.84	1.2	13.7	20

Conclusions

The case study considered is very difficult one for many reasons: uncertainty with temporal behavior of source term, complicated atmospheric dispersion, uncertainties with environmental parameters defining dry and especially wet deposition, very high local variability of fallout, etc. Before beginning of the study, it was clear that science based model can only predict spatial trends of the fallout. But the reality is even more difficult. Atmospheric model parameterization used is far from being optimal even after many trials and tunings. Obtained results differ significantly from measured ones, but the spatial pattern seems to be caught – the position of the main trace is presented well by a model. Limited knowledge in parameterization of the model can be avoided by using additional information inserted in measured values. Hybrid approach can improve obtained result. But when there is a lot of measurements and limited knowledge about atmospheric model parameters it is easier to apply directly a data driven model. In fact, hybrid models (atmospheric+geostat/ANN) can be useful when there are not enough data measurements, e.g. short and intermediate time after an accident. Nevertheless, such comprehensive studies are extremely useful to understand underlying phenomena and to develop science based models. Moreover, science based models calibration using spatial information is far more advanced approach than usual tuning of parameters.

Acknowledgments

The work is partly supported by INTAS grant 99-00099 and crdf grant RG2-2236.

References

1. Kostikov, A.A., M.A. Novitski. Numerical Modeling of Admixture Dispersion from a Point Source Under Condition of Breeze Circulation. Proc. of IEM, N 37(120), 1986, p. 25-38. (in Russian).
2. Boughton, B.A., J.M.Delauentis, W.E.Dunn. A Stochastic Model of Particle Diffusion in the Atmosphere. // Boundary Layer Meteor., 1987.-v.40, pp. 147-163.
3. Martens, R., K.Mabmeyer, W.Pfeffer et al. Besendsaufnahme und Bewertung der Perzeit Genutzen //Report GRS Mai 1987.
4. Pasler-Sauer J. Comparative Calculations and Validation Studies With Atmospheric Dispersion Models. //Report KfK 4164, November 1986, 130 p.
5. Arutunjan, R.V., V.V. Belikov, G.V.Belikova et al. Models of Radionuclides Transport in Atmosphere from Integrated Software Package "Nostradamus". //Preprint NSI-31,1994a.
6. Arutunjan, R.V, V.V.Belikov, G.V.Belikova et al. New Efficient Numerical Procedures of Modeling the Radionuclide Propagation in the Atmosphere and Their Practical Implementation. Applied Energy: Russian Journal of Fuel, Power and Heat Systems, 1995a, V.33, N4, p.22-33
7. J.B. Klemp, R.B. Wilhelmson (1978) *The simmulation of three-dimensional convetctive storm dynamics.* J. of the atmospheric scienc.v.35,N 6, p. 1070 -1096 .
8. Terner J. Effects of buoyancy in liquids.- M.: Mir, 1977.- 430 pp.
9. J.E. Penner, L.C. Haselman (1985) *Smoke inputs to climate models*. Lauwrence Livermore National Laboratory report UCRL-92523.
10. G.J. Tripoli, W.R. Cotton (1982) *The Colorado State University three dimensional cloud / mesoscale model, Part 1 : general theoretical framework and sensitivity experiments.* J. Rech. Atmos., 16, p. 185 - 220 .
11. J.E Penner, L.C Haselman, L.L. Edwards (1986) *Smoke-Plume distributions above large-scale fires: Implications for simulations of "Nuclear winter".* J. of Climate and Appl. meteor.v.25, N 10, p. 1434-1444.
12. Consequences of nuclear war: physical and atmospheric effects (1998). M.: Mir , pp.392. (in Russian)
13. S.R. Hanna (1989) *Prediction and observed colling tower plume rise and visible plume lengs.* J. Atmos. Envir. v10,N2
14. Orlov, M.Yu., Snykov V.P., Khvalensky Yu. A. et al. *Radioactive contamination of Belarus and Russia territories after Chernobyl accident.* Atomic Energy №72, issue 4, 1992, p.371-376.
15. Haykin, S., 1999. *Neural Networks. A Comprehensive Foundation*. Second Edition. Prentice Hall International, Inc.